Paper No. 407. (quote when citing this article)
Eleventh World Conference on Earthquake Engineering
ISBN: 0 08 042822 3

DYNAMIC TESTING OF FULL-SCALE STEEL MOMENT CONNECTIONS

C.M. UANG and D.M. BONDAD

Division of Structural Engineering, University of California, San Diego
La Jolla, CA 92093-0085, USA

ABSTRACT

The effects of strain rate on the brittle fracture of steel moment frame connections discovered after the 1994 Northridge earthquake was investigated experimentally. Five full-scale specimens were tested to failure -- three tested statically and two tested dynamically. The connections details and welding procedure followed pre-Northridge design practice. It was found that dynamically loaded specimens tended to have lower plastic rotation and energy dissipation capacities. The failure mode also differed; fracture propagated into the column flange for the dynamically, but not the statically, loaded specimens. Recorded strain readings indicated that the level of strain rate increased the force demand in the beam flange groove weld by about 10%

KEYWORDS

steel frame connections, strain rate effects, dynamic testing, ATC-24 protocol, brittle fracture, Northridge earthquake

INTRODUCTION

The 1994 Northridge earthquake resulted in widespread, and unexpected, damage to steel moment frames. While the special steel moment-resisting frame (SMRF) was designed to dissipate energy through the stable yielding of the beam and column panel zone, in reality, this was not the case. Instead, brittle fracture was prevalent, with the most common occurrences being crack propagation in weldments, the heat affected zones in beam and column flanges, and webs.

Previous testing of large-scale moment connections has been done quasi-statically (Popov et al. 1985, Engelhardt and Husain, 1993, Tsai et al. 1995), which effectively removes any strain rate effects. While this makes the testing procedure simpler, it has raised questions as to its appropriateness to seismic applications. Because of the poor performance of steel SMRF's observed after the Northridge earthquake, the effect of strain rate, especially with respect to crack initiation and propagation, needs to be investigated.

OBJECTIVE

The overall objective of this research was to investigate the cyclic performance of pre-Northridge moment connections and to test promising repair schemes. This paper will focus on the effects of strain rate on plastic deformation capacity, energy dissipation, failure mode, and forced demand to weldments, of pre-Northridge moment connections.

TEST SPECIMENS AND TESTING PROCEDURES

Design, Fabrication, and Material Properties

A total of five identical specimens were built and tested, using the test setup pictured in Fig. 1. Three specimens were tested using conventional quasi-static testing procedures. The remaining two were tested dynamically in order to include strain rate effects. While each specimen was then repaired and retested, only the first series of results are presented here.

The moment connection designed per pre-Northridge design practice is illustrated in Fig. 2. All the specimens were fabricated by a commercial fabricator. Because of the importance of simulating actual building construction, the specimens were constructed under field conditions. All welding followed the welding procedure specifications to reflect the pre-Northridge practice.

Self-shielded flux core arc welding was used on the test specimens. The 3 mm (0.120 in.) diameter E70-4 electrode was used for making the field groove welds, and the 1.8 mm (0.072 in.) diameter E71T-8 electrode was used for making the supplemental beam web welds.

To minimize the variables that would affect a direct comparison between the static and dynamic test results, both the beams and columns were from the same heats of steels. Steel coupons were taken from the A36 steel beam and A572 Grade 50 steel column. The results from the ASTM tests are found in Table 1. Also noted are the results from Charpy V-Notch tests performed on six test specimens taken from the steel column.

Loading Sequence

For the quasi-static tests, the ATC-24 (1992) testing protocol (see Fig. 3a) was adopted. Three complete loading cycles, with displacement amplitudes in multiples of yield displacement, δ_y, were applied to each specimen. This expected δ_y was determined from a nonlinear analysis using DRAIN-2DX (1993), which was performed before the tests. A value of δ_y = 3.56 cm was used.

For dynamic tests, no testing protocol similar to ATC-24 existed. In order to compare the response between static and dynamic tests, it was decided to establish a dynamic loading sequence based on the ATC-24 protocol. The displacement time history, shown in Fig. 3b to simulate a structural response with a period of 1 sec. and a maximum story drift ratio of 3%, was imposed to the beam tip of specimens UCSD-4 and -5. (A response period of 1 sec. was selected to simulate a steel moment frame about four to six stories in height. A 3% story drift ratio was assumed to be typical of that produced by severe design earthquakes.)

RESULTS

Global Response

The beam tip displacement versus load relationships for two of the quasi-static and both the dynamic specimens are illustrated in Fig. 4. Specimen UCSD-1 performed the most poorly of all the statically tested specimens, not even completing a single cycle at the $2\delta_y$ displacement amplitude. Specimen UCSD-2 failed during the negative excursion of the first $3\delta_y$ cycle. The performance of specimen UCSD-3 (not shown) is very similar to that of UCSD-2.

While quasi-static tests were stopped as soon as fracture occurred, this was not the case for the dynamic testing. The hysteresis loops of specimens UCSD-4 and -5 show severe pinching behavior and a drastic drop in capacity upon fracture. (Specimen UCSD-4 shows pinching behavior on one side because only one flange fractured.)

Plastic Rotation and Energy Dissipation Capacity

The relationships between moment and total plastic rotation, which includes beam and panel zone components, of the test specimens are illustrated in Fig. 5. At the onset of beam flange fracture, the total plastic rotation achieved in each specimen, as well as the contribution from panel zone yielding, are shown in Fig. 6; the hysteresis energy dissipation capacities are also shown. Based on this very limited database, the figure appears to suggest that, on average, the plastic deformation and energy dissipation capacities are reduced by strain rate effects.

Failure Modes

Table 2 summarizes the failure mode observed in each specimen. Prior to fracture, every test specimen experienced shear yielding in the column panel zone as evinced by flaking of the whitewash and strain gage readings.

It is noted that fracture could occur in the weld metal or in the fusion zone between the groove weld and column face or beam flange. It is also interesting to note that fracture, which might have been initiated at the root pass of the groove weld above the backup bar, extended into the column flange for the dynamically tested specimens. (See Fig. 7(b) for the propagation of the crack from the root of the groove weld into the column flange.) Such a failure mode, which was more difficult to repair, was not observed in any of the three statically tested specimens. The shear plate connecting the beam web and column flange was also severely damaged for both dynamically tested specimens (see Fig. 7(a)).

Strain Rate Effects

Based on the reading of a strain gage placed on the center of the beam bottom flange (3.81 cm away from the column face), the strain rate was computed and is shown in Fig. 8. The figure indicates that a strain rate on the order of 10^{-1} cm/cm/sec. was reached. The increase in the yield stress for such a magnitude of strain rate was about 10% (Moncarz and Krawinkler 1981). The increase in the strength of beam flange in turn represents an increase of force demand to the groove weld. That is, strain rate increases the force demand to the groove weld. Since it is well known that strain rate reduces the notch toughness of groove welds (Barsom and Rolfe 1987), the combined effects make the welded groove joint of the pre-Northridge moment connection more vulnerable to brittle fracture under dynamic loading conditions.

CONCLUSIONS

Based on the test results of three statically loaded and two dynamically loaded full-scale steel moment frame connections designed per pre-Northridge practice, the following conclusions can be made.

(1) The seismic performance (plastic rotation and energy dissipation capacities) of the dynamically loaded specimens appeared to be in the range of the lower bound of statically loaded specimens.

(2) Fracture of beam flange groove welds propagated into the column flange for dynamically loaded specimens. This phenomenon, which was not observed in the statically loaded specimens, suggested that loading rate might affect the fracture pattern.

(3) The strain rate of dynamically loaded beam flanges was on the order of 10^{-1} cm/cm/sec. As a result, the increase in force demand to the groove weld was about 10%.

ACKNOWLEDGEMENTS

Static testing was sponsored by the SAC Joint Venture and dynamic testing was sponsored by the National Science Foundation. The authors also would like to thank Bannister Steel, Asbury Steel, Baresel Co., Hassett Engineering, and the Northridge Steel Industry Fund for their contribution to the projects.

REFERENCES

ATC-24 (1992). *Guidelines for cyclic seismic testing of components of steel structures for buildings.* Applied Technology Council. Redwood City, Calif.

Barsom, J.M. and S.T. Rolfe (1987). *Fracture & fatigue control in structures.* Prentice Hall, New Jersey.

Engelhardt, M.D., and A.S. Husain (1993). "Cyclic-loading performance of welded flange-bolted web connections." *J. Struct. Engrg.*, ASCE, Vol. 119, No. 12, pp. 3537-3550.

Moncarz, P.D. and H. Krawinkler (1981). Theory and application of experimental model analysis in earthquake engineering. *Report No. 50*, J.A. Blume Earthquake Engrg. Ctr., Stanford Univ., Calif.

Popov, E.P., N.R. Amin, J.C. Louie, and R.M. Stephen (1985). "Cyclic behavior of large beam-column assemblies." *Earthquake Spectra,* EERI, Vol. 1, No. 2, pp. 203-238.

Prakash, V., G.H. Powell, and F.C. Filippou (1993). DRAIN-2DX. *User Guide*, Univ. of Calif., Berkeley, Calif.

Tsai, K.C., K. Wu, and E.P. Popov (1995), "Experimental performance of seismic steel beam-column moment joints." *J. Struct. Engrg.*, ASCE, Vol. 121, No. 6, pp. 925-931.

Table 1. Material Characteristics

Member	Steel Type		Fy (MPa)	Fu (MPa)	Elongation (%)
Beam W30X99	A36	Flange	320.6	466.8	31.3
		Web	393.7	499.9	25.0
Column W14X176	A572 Grade 50	Flange	362.0	470.2	32.0
		Web	353.0	463.3	30.5

NOTE: Average toughness from the Charpy V-Notch tests was 180 J @ 21°C.

Table 2. Observed Fracture Mode

Specimen	Observed Fracture Mode
UCSD-1	beam bottom flange (between groove weld and column face)
UCSD-2	beam top flange (between groove weld and beam flange)
UCSD-3	beam top flange (in groove weld)
UCSD-4	beam bottom flange (fracture between groove weld and column face propagated into column flange)
UCSD-5	beam top and bottom flanges between groove weld and column face (fracture on the beam bottom flange propagated into column flange)

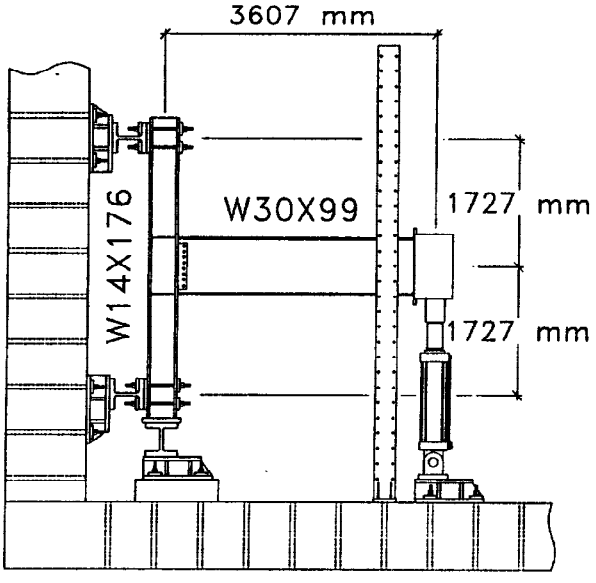

Fig. 1. Test Setup

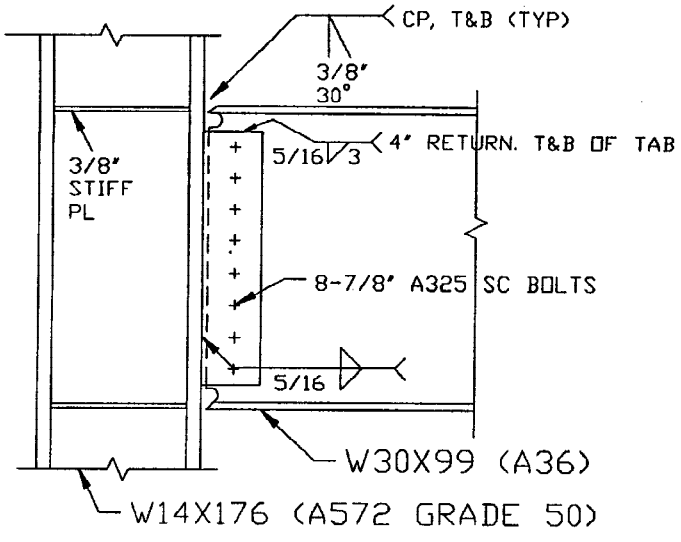

Fig. 2. Pre-Northridge Connection Details

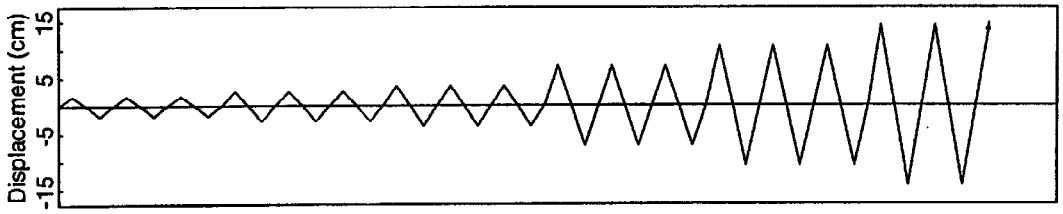

(a) Static Test (ATC-24)

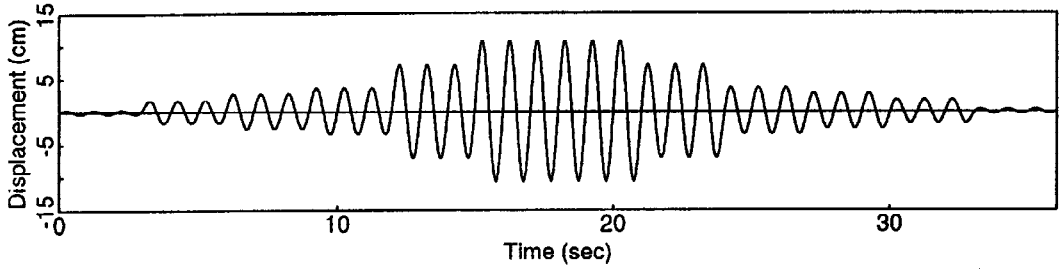

(b) Dynamic Test

Fig. 3. Loading Sequences

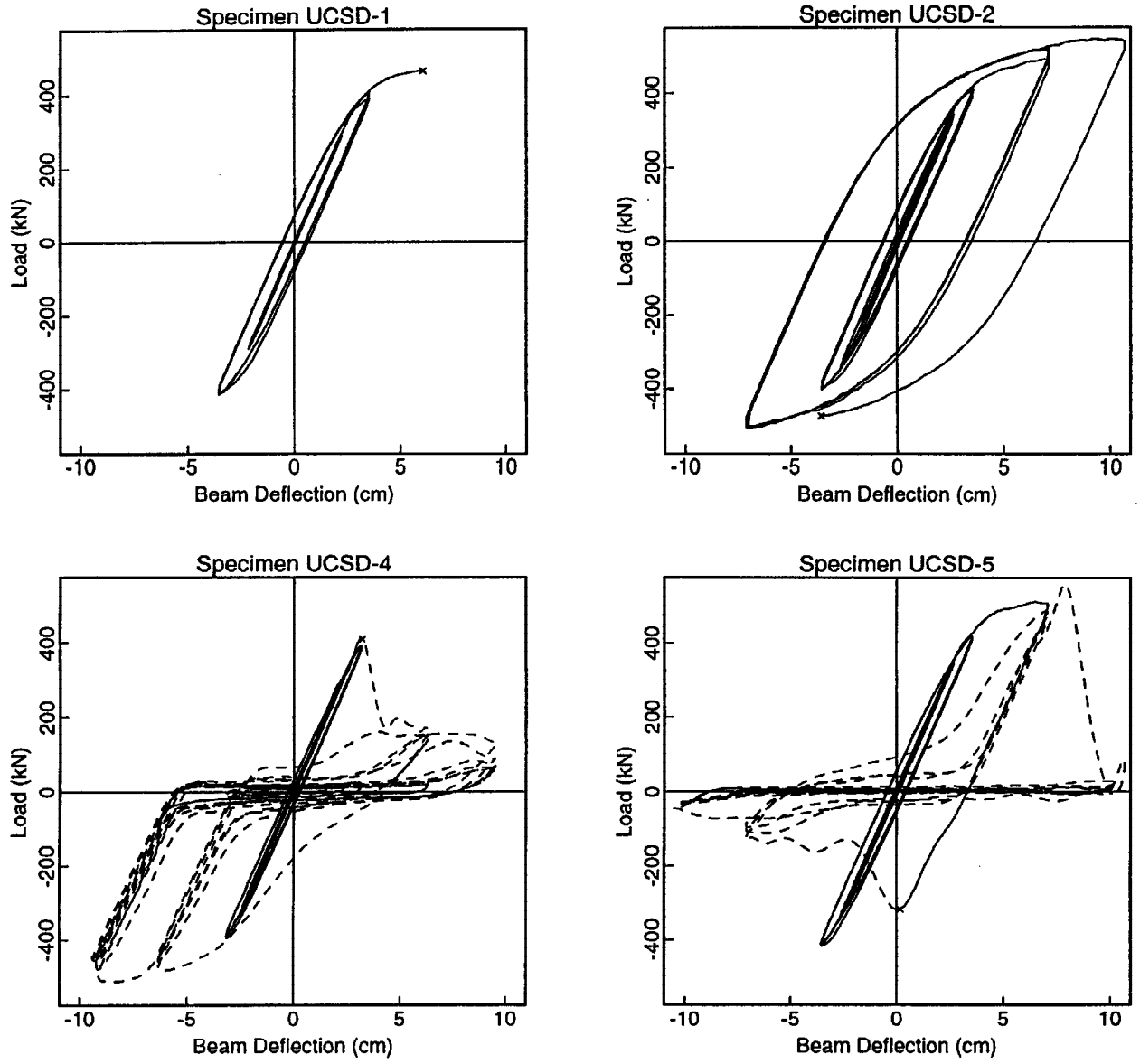

Fig. 4. Load versus Beam Tip Deflection Relationship

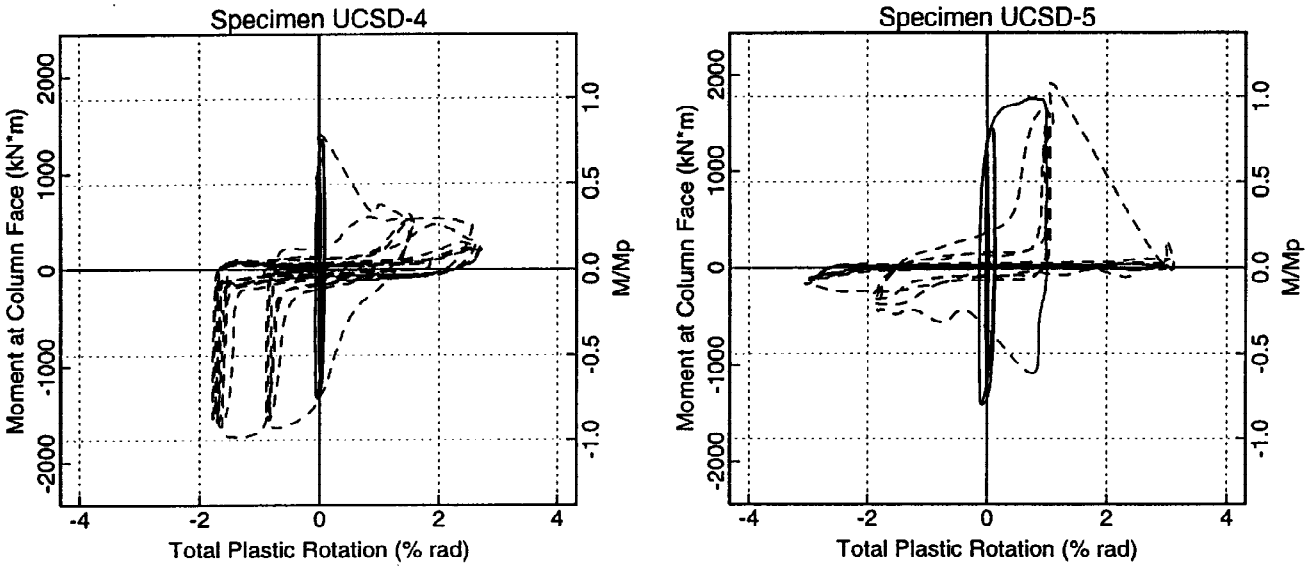

Fig. 5. Moment versus Total Plastic Rotation Relationship

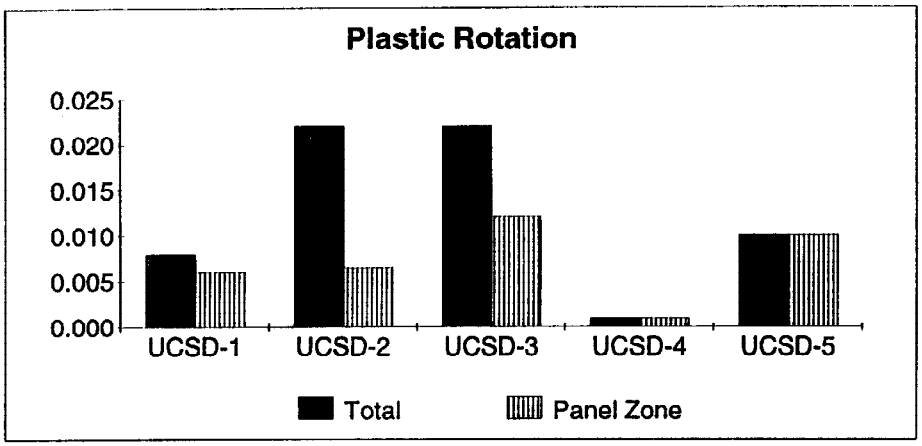

(a) Plastic Rotation

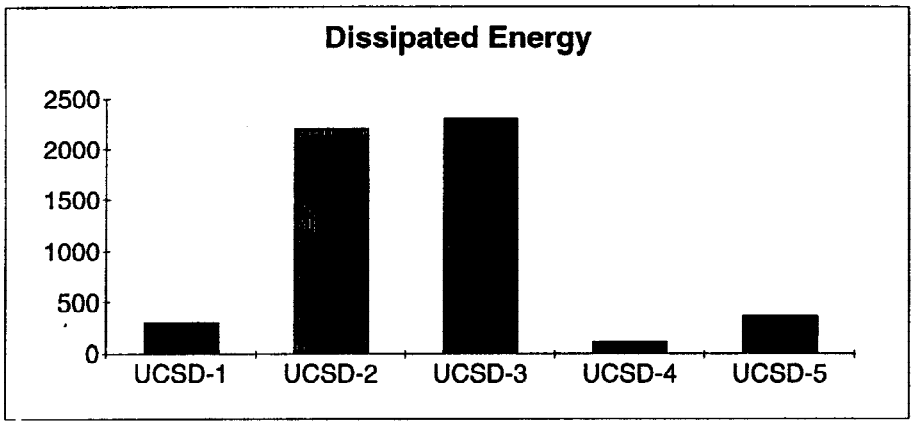

(b) Hysteretic Energy Dissipation

Fig. 6. Comparison of Plastic Rotation and Energy Dissipation Capacities

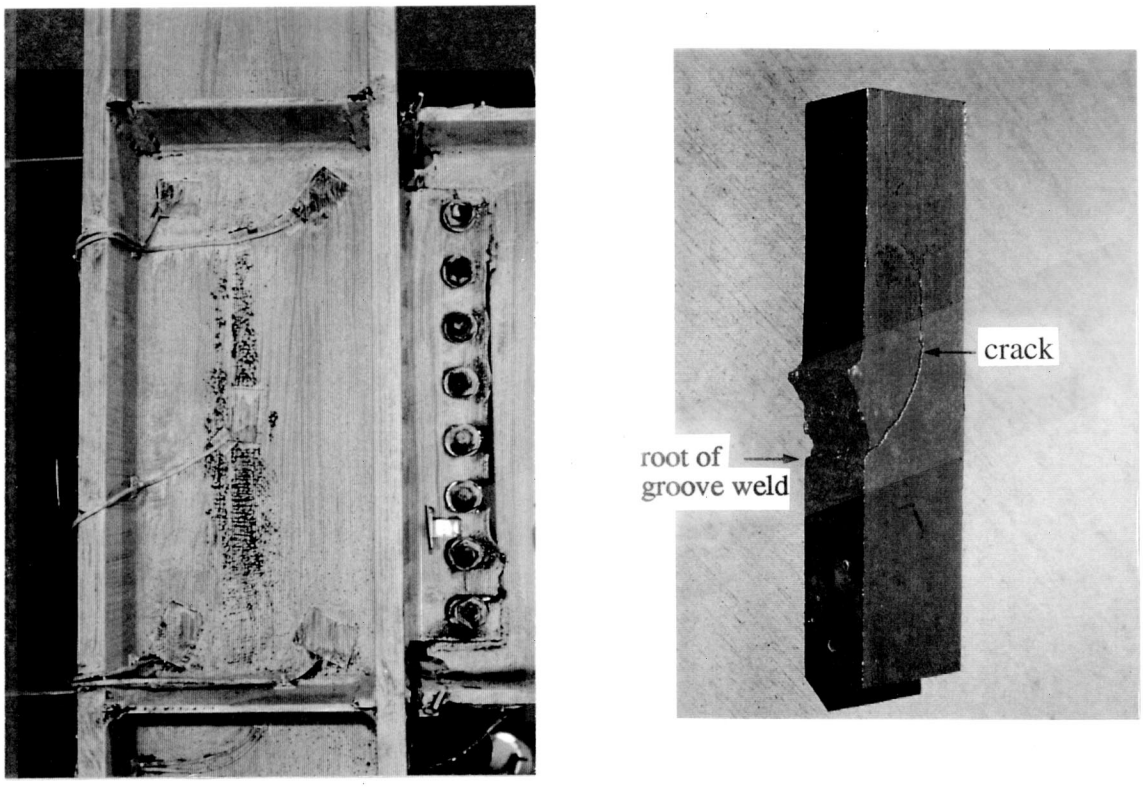

(a) fracture of beam bottom flange (b) crack in column flange

Fig. 7. Failure Mode of Specimen UCSD-4

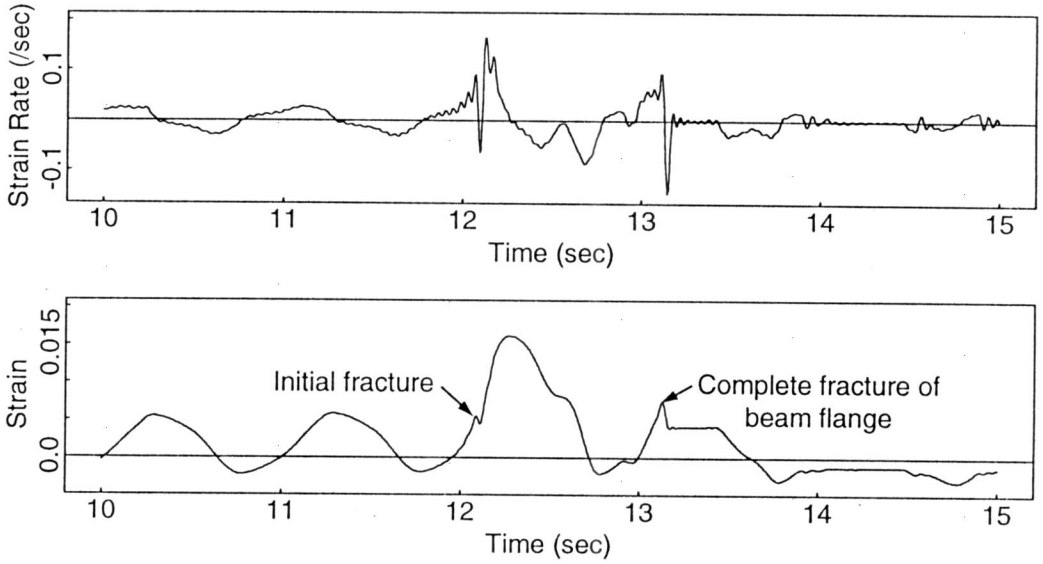

Fig. 8. Beam Bottom Flange Strain and Strain Rate Time Histories (Specimen UCSD-4)